Supplementary Information for Charge Carrier Mobilities in γ-Graphynes: A computational approach

Elif Unsal*

Institute for Materials Science and Nanotechnology, TU Dresden, 01062, Dresden, Germany. and Institute of Physical Chemistry, Friedrich-Schiller-Universität, 07743, Jena, Germany.

Alessandro Pecchia

CNR-ISMN, Via Salaria km 29.300, 00015 Monterotondo Stazione, Rome, Italy.

Alexander Croy

Institute of Physical Chemistry, Friedrich-Schiller-Universität, 07743, Jena, Germany.

Gianaurelio Cuniberti†

Institute for Materials Science and Nanotechnology, TU Dresden, 01062, Dresden, Germany. and Dresden Center for Computational Materials Science (DCMS), TU Dresden, 01062, Dresden, Germany.

(Dated: September 22, 2025)

CONTENTS

* elif.unsal@tu-dresden.de

† gianaurelio.cuniberti@tu-dresden.de

I. STRUCTURAL AND ELECTRONIC PROPERTIES

TABLE I. Calculated structural properties: the lattice constant a, the bond lengths (aromatic, single, and triple), and the 2D mechanical moduli (Y_{2D}, B_{2D}, and μ_{2D}).

		a [Å]	sp^2-sp^2 [Å]	sp^2-sp [Å]	sp-sp [Å]	Y_{2D} [N/m]	B_{2D} [N/m]	μ_{2D} [N/m]
Graphene	DFTB-mio-1-1	2.47	1.42	-	-	375	250	150
	DFT-PBE	2.47	1.43	-	-	328	217	132
	DFT-PBE (Ref.)	-	-	-	-	-	-	-
GY	DFTB-mio-1-1	6.92	1.41	1.43	1.22	174	176	58
	DFT-PBE	6.89	1.43	1.41	1.22	168	141	60
	DFT-PBE (Ref. [1])	6.89	1.43	1.41	1.22	166	-	-
GDY	DFTB-mio-1-1	9.53	1.42	1.43	1.23	141	117	50
	DFT-PBE	9.46	1.43	1.40	1.23	116	99	41
	DFT-PBE (Ref. [2])	9.48	-	-	-	-	-	-

TABLE II. Calculated electronic properties: band gap (E_{gap}) and effective masses (m_e^*, m_h^*) along $M-\Gamma$ and $M-K$.

			$M-\Gamma$	$M-K$
		E_{gap} [eV]	m_e^*, m_h^* [m_0]	m_e^*, m_h^* [m_0]
GY	DFTB-mio-1-1	1.38	0.30, -0.32	0.24, -0.26
	DFT-PBE	0.46	0.20, -0.22	0.08, -0.09
	DFT-PBE (Ref. [1])	0.46	0.20, -0.22	0.08, -0.09
GDY	DFTB-mio-1-1	1.52	0.28, -0.32	0.28, -0.32
			0.18, -0.20	0.19, -0.21
	DFT-PBE	0.48	0.09, -0.09	0.09, -0.09
			0.07, -0.07	0.07, -0.07
	DFT-PBE (Ref. [2])	0.46	-	-

II. PARAMETRIZATION TEST

Calculations were performed using the open source DFTB+ code [3]. In order to better gauge the effect of the parametrization of the Hamiltonian matrix elements on our results, we used different Slater–Koster sets: 3ob-3-1 [4] 3ob:freq [5] mio-1-1 [6] ob2-1-1 [7] and matsci-0-3 [8]. We performed a geometry optimization using the SCC method [6].

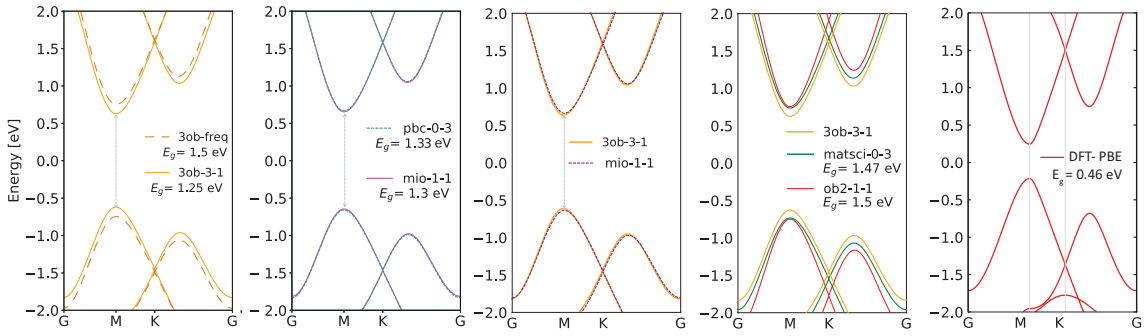

FIG. 1. Calculated electronic band structures with different Slater-Koster parametrizations.

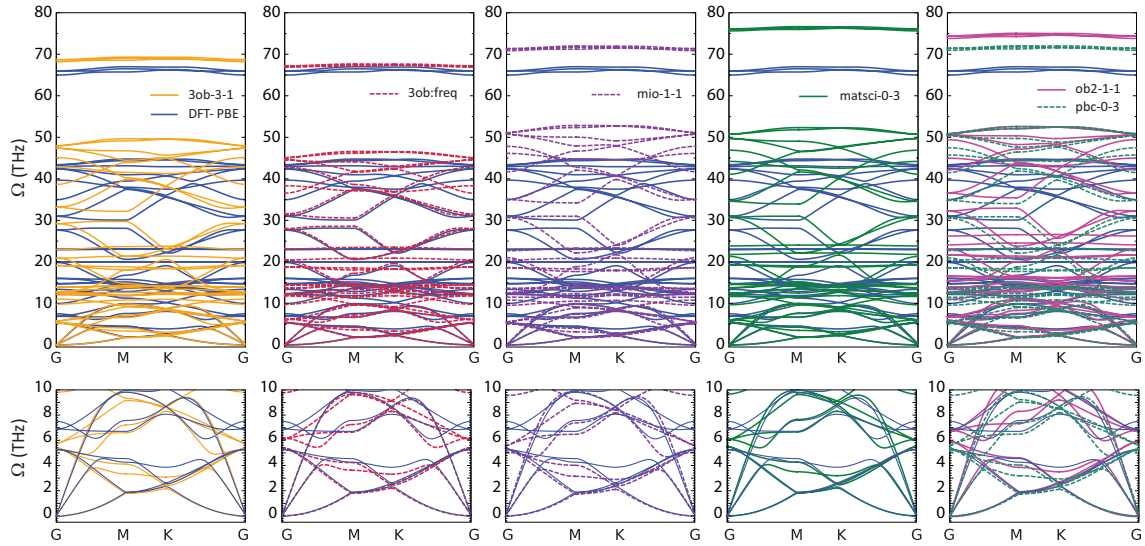

FIG. 2. Calculated phonon band structures with different Slater-Koster parametrizations.

III. KANE-BAND MODEL

For a 2D Kane-band, the electronic dispersion is described by:

$$\varepsilon + \alpha\varepsilon^2 = \frac{\hbar^2\mathbf{k}^2}{2m^*}, \tag{1}$$

where α is the non-parabolicity parameter, $\hbar$ is the reduced Planck constant and m^* is the effective mass of the charge carriers. Here, $\mathbf{k}^2$ is the squared wave vector in 2D, $k_x^2 + k_y^2$. After rearranging and solving for ε, it can be explicitly written as a function of $\mathbf{k}$

$$\varepsilon = \left(\frac{\hbar^2\mathbf{k}^2}{2m\alpha} + \frac{1}{4\alpha^2}\right)^{\frac{1}{2}} - \frac{1}{2\alpha}. \tag{2}$$

a. Carrier Velocity Group velocity of the charge carriers along a certain direction, for instance, in x-direction, is defined as the rate of change of the energy ε with respect to the wave vector $\mathbf{k}$, scaled by the $\hbar$.

$$v_x = \frac{1}{\hbar}\frac{\partial\varepsilon(\mathbf{k})}{\partial k_x} \tag{3}$$

$$= \frac{1}{2\hbar}\left[\frac{\hbar^2\mathbf{k}^2}{2m\alpha} + \frac{1}{4\alpha^2}\right]^{-\frac{1}{2}}\frac{2k_x\hbar^2}{2m\alpha} \tag{4}$$

$$= \frac{\hbar k_x}{2m\alpha}\left[\frac{\hbar^2\mathbf{k}^2}{2m\alpha} + \frac{1}{4\alpha^2}\right]^{-\frac{1}{2}} \tag{5}$$

Now, we rearrange the Eq.2

$$\left(\frac{\hbar^2\mathbf{k}^2}{2m\alpha} + \frac{1}{4\alpha^2}\right)^{\frac{1}{2}} = \frac{2\alpha\varepsilon + 1}{2\alpha} \tag{6}$$

and use this in the Eq.5 in order to define velocities in terms of α and energy ε:

$$v_x = \frac{\hbar k_x}{2m\alpha}\left(\frac{2\alpha}{2\alpha\varepsilon + 1}\right) = \frac{\hbar k_x}{m}\left(\frac{1}{2\alpha\varepsilon + 1}\right) \tag{7}$$

b. Charge Carrier Density The charge carrier density n_C in 2D at a specific temperature T and chemical potential μ is given by

$$n_C = \frac{1}{A_{uc}}\sum_n \int \frac{d^2\mathbf{k}}{\Omega_{BZ}}\left[f^0(\varepsilon_n;\mu,T) - f^0(\varepsilon_n;\varepsilon_F,0)\right], \tag{8}$$

where A_{uc} is the unit cell area and Ω_{BZ} is the Brillouin Zone area, $\Omega_{BZ} = 4\pi^2/A_{uc}$. $f^0(\varepsilon;\mu,T)$ is the Fermi distribution function. For the differential area element $d^2\mathbf{k}$ in polar coordinates, we used $2\pi k dk$ accounting for the integration over the angular component:

$$n_C = \frac{1}{4\pi^2}\sum_n \int 2\pi k dk \left[f^0(\varepsilon_n;\mu,T) - f^0(\varepsilon_n;\varepsilon_F,0)\right]. \tag{9}$$

where the summation over n accounts for contributions from the bands. The carrier densities for electrons $n_C = n_e$ and holes $n_C = n_h$ are obtained by summing over the conduction and valence bands, respectively. Then we have

$$n_C = \frac{1}{4\pi^2}\int 2\pi k dk \left[f^0(\varepsilon;\mu,T) - f^0(\varepsilon;\varepsilon_F,0)\right]. \tag{10}$$

By using the Eq.1, we can use an expression for $\mathbf{k}$

$$k = \frac{\sqrt{2m}}{\hbar}\sqrt{\varepsilon(1+\alpha\varepsilon)}, \tag{11}$$

and differentiate it with respect to ε in order to convert the integral from momentum space to energy space.

$$dk = \frac{\sqrt{2m}}{\hbar}\left[\frac{1}{2}(\varepsilon+\alpha\varepsilon^2)^{-\frac{1}{2}}(1+2\alpha\varepsilon)\right]d\varepsilon \tag{12}$$

$$= \frac{\sqrt{2m}}{2\hbar}\frac{(1+2\alpha\varepsilon)}{\sqrt{(\varepsilon+\alpha\varepsilon^2)}}d\varepsilon \tag{13}$$

Next, we substitute the expressions for k and dk in to Eq.10 to rewrite the integral for carrier densities

$$n_C = \frac{1}{2\pi}\int \frac{1+2\alpha\varepsilon}{2\alpha}\frac{2m\alpha}{\hbar^2}d\varepsilon\left[f^0(\varepsilon;\mu,T) - f^0(\varepsilon;\varepsilon_F,0)\right] \tag{14}$$

$$= \frac{m}{2\pi\hbar^2}\int d\varepsilon(1+2\alpha\varepsilon)\left[f^0(\varepsilon;\mu,T) - f^0(\varepsilon;\varepsilon_F,0)\right]. \tag{15}$$

c. Electrical Conductivity Within the Boltzmann transport framework [9], conductivity tensor in 2D is defined as

$$\sigma_{xy} = \frac{e^2}{A_{uc}}\sum_n \int \frac{d^2\mathbf{k}}{\Omega_{BZ}}\left[-\frac{\partial f^0(\varepsilon_n;\mu,T)}{\partial\varepsilon}\right] v_{xn}v_{yn}\tau_n, \tag{16}$$

where energies ε_n, velocities v_n and relaxation times τ_n are as a function of $\mathbf{k}$. After summing over the bands, conductivity tensor σ_{xy} can be written as

$$\sigma_{xy} = \frac{e^2}{A_{uc}} \int \frac{d^2\mathbf{k}}{\Omega_{BZ}} \left[-\frac{\partial f^0(\varepsilon;\mu,T)}{\partial \varepsilon} \right] v_x v_y \tau. \tag{17}$$

After inserting $\Omega_{BZ} = 4\pi^2/A_{uc}$, $d^2\mathbf{k} = 2\pi k dk$ and the velocities as in Eq. 7, we get

$$\sigma_{xy} = \frac{e^2}{2\pi} \sum_{x,y} \int k dk \left[-\frac{\partial f^0(\varepsilon;\mu,T)}{\partial \varepsilon} \right] \frac{\hbar k_x}{m(1+2\alpha\varepsilon)} \frac{\hbar k_y}{m(1+2\alpha\varepsilon)} \tau. \tag{18}$$

The two-dimensional conductivity σ_{2D} is obtained by averaging the trace of the conductivity tensor

$$\sigma_{2D} = \frac{1}{2} tr(\sigma) = \frac{1}{2} \sum_{i=1}^{2} \sigma_{ii}. \tag{19}$$

Since we are only taking the trace, we have $\rightarrow (k_x^2 + k_y^2)/2 = \mathbf{k}^2/2$. We can re-write σ_{2D} as

$$\sigma_{2D} = \frac{e^2}{2\pi} \int k dk \left[-\frac{\partial f^0(\varepsilon;\mu,T)}{\partial \varepsilon} \right] \frac{\hbar^2}{m^2(1+2\alpha\varepsilon)^2} \frac{\mathbf{k}^2}{2} \tau. \tag{20}$$

Then we change the variable k to ε using the following relations.

$$k dk = (1+2\alpha\varepsilon) \frac{m}{\hbar^2} d\varepsilon \tag{21}$$

$$\frac{\mathbf{k}^2}{2} = \frac{m}{\hbar^2} \varepsilon(1+\alpha\varepsilon) \tag{22}$$

We substitute these relations in Eq. 20 and obtain

$$\sigma_{2D} = \frac{e^2}{2\pi} \int (1+2\alpha\varepsilon) \frac{m}{\hbar^2} d\varepsilon \left[-\frac{\partial f^0(\varepsilon;\mu,T)}{\partial \varepsilon} \right] \frac{\hbar^2}{m^2(1+2\alpha\varepsilon)^2} \frac{2m}{\hbar^2} (\varepsilon + \alpha\varepsilon^2) \tau. \tag{23}$$

After simplifying the expression, we arrive at the final form of 2D conductivity within the Kane-band model

$$\sigma_{2D} = \frac{e^2}{2\pi\hbar^2} \int d\varepsilon \left[-\frac{\partial f^0(\varepsilon;\mu,T)}{\partial \varepsilon} \right] \frac{(\varepsilon + \alpha\varepsilon^2)}{(1+2\alpha\varepsilon)} \tau. \tag{24}$$

The charge carrier densities and electrical conductivity are linearly proportional to the temperature in the parabolic band limit, as α goes to zero. Therefore, the analytical solutions for mobility do not depend explicitly on temperature. When the Kane band approximation is employed, we can see that the charge carrier densities are shifted by $2\alpha\varepsilon$, and the electrical conductivities are no longer linearly related to energy ε, as seen in Eqs. (15) and (24). Therefore, the conductivity and charge carrier density ratio no longer gives a constant and is explicitly temperature-dependent. Therefore, the Kane band model allows for investigating how mobility changes with temperature within the constant relaxation time approximation.

IV. NON-PARABOLICITY IN GRAPHYNES

It is commonly assumed that electronic bands exhibit parabolic dispersion near the band edges. However, deviations from this parabolicity can have a significant impact on the transport properties of materials [10, 11]. In this study, we employed the quasi-linear Kane-band model[12] to investigate nonparabolic effects in graphynes. The non-parabolicity parameter α was determined by fitting the energy dispersion near the band edges.

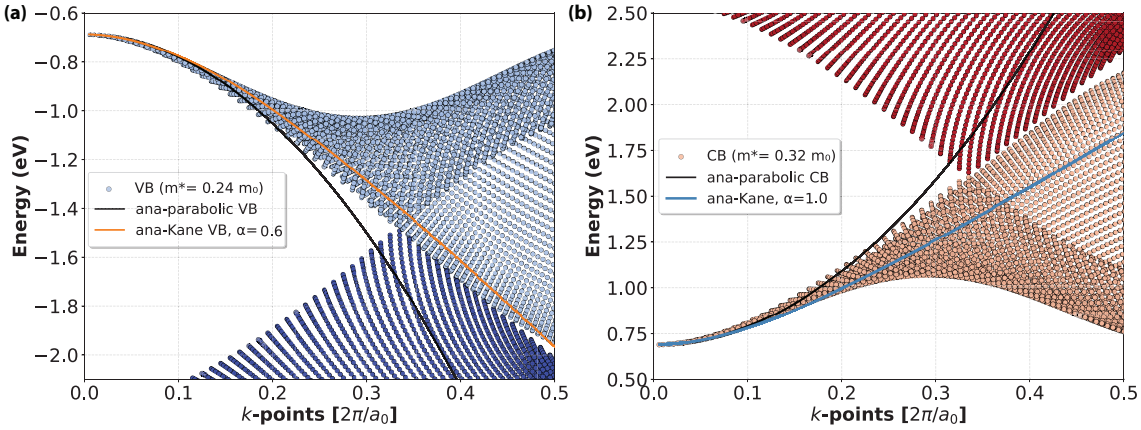

FIG. 3. (a) Valence and (b) conduction bands graphyne (GY), with the analytical parabolic and Kane bands.

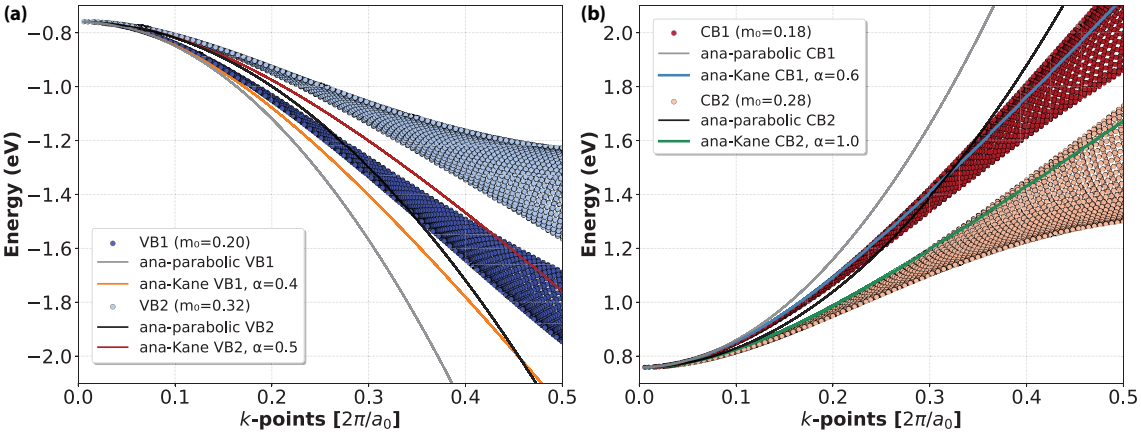

FIG. 4. (a) Valence and (b) conduction bands in graphdiyne (GDY), with the analytical parabolic and Kane bands.

V. DENSITIES AND ELECTRICAL CONDUCTIVITIES

The densities and conductivities calculated using DFTBephy, along with the analytical values obtained based on the parabolic and Kane-band models, are presented in Figures 5 and 6. Due to the band-edge degeneracy of the conduction and valence bands in GDY, contributions from these degenerate bands have been taken into account in the density and conductivity calculations. The conductivity values shown in the figures represent the trace $\sigma_x + \sigma_y$.

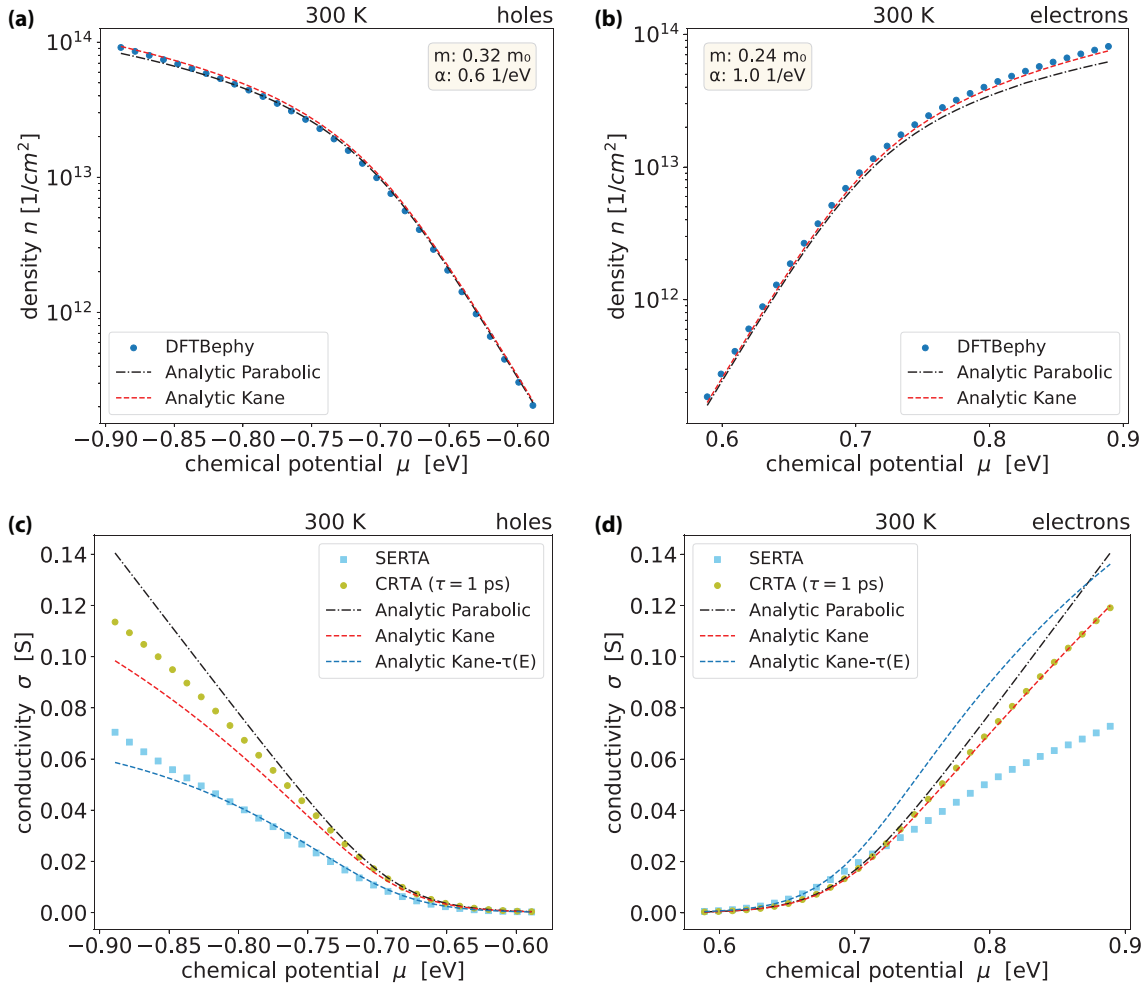

FIG. 5. Densities for (a) holes and (b) electrons graphyne (GY). Effective mass m and non-parabolicity parameter α values are annotated in the figure. Conductivity values for (c) holes and (d) electrons.

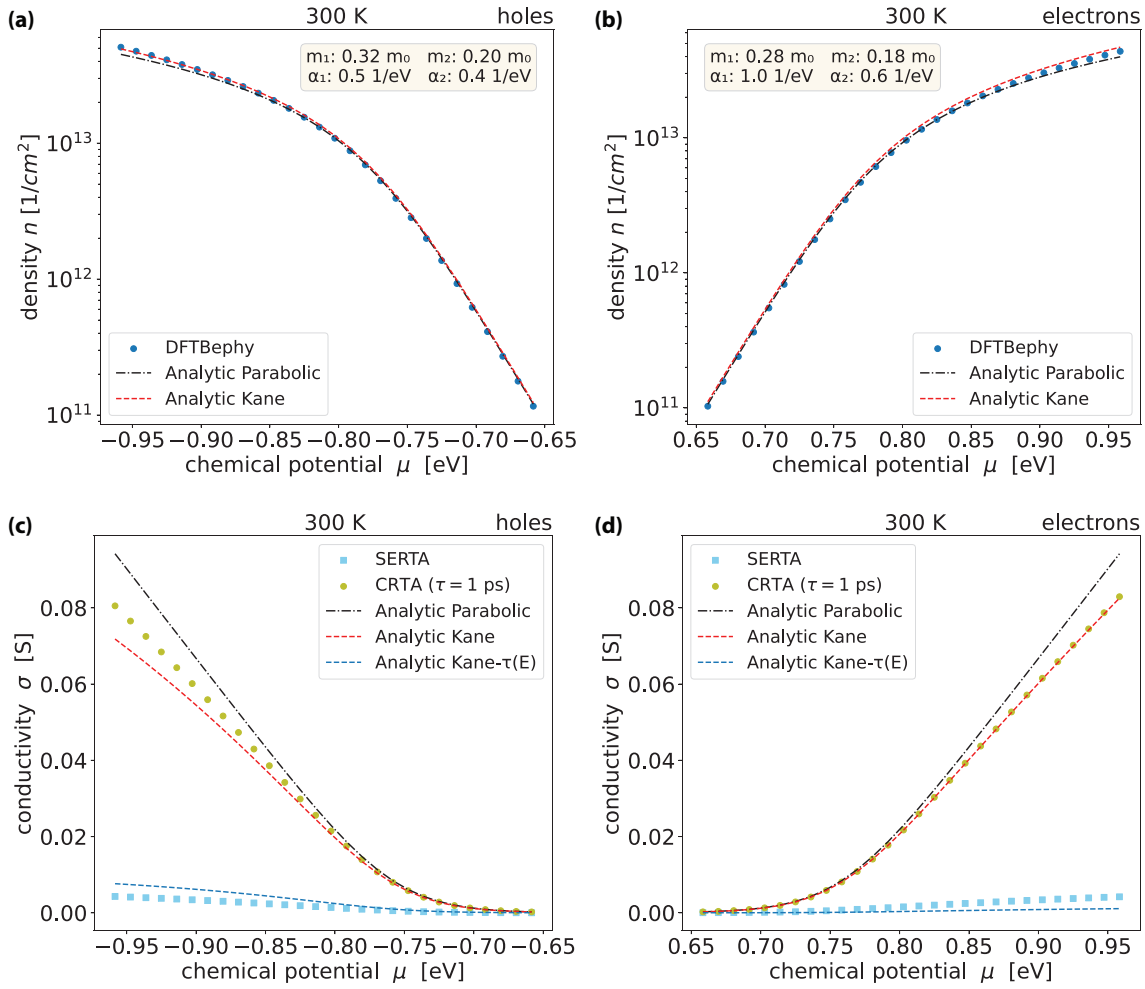

FIG. 6. Densities for (a) holes and (b) electrons graphdiyne (GDY). Effective mass m and non-parabolicity parameter α values are annotated in the figure. Conductivity values for (c) holes and (d) electrons.

VI. SCATTERING RATES

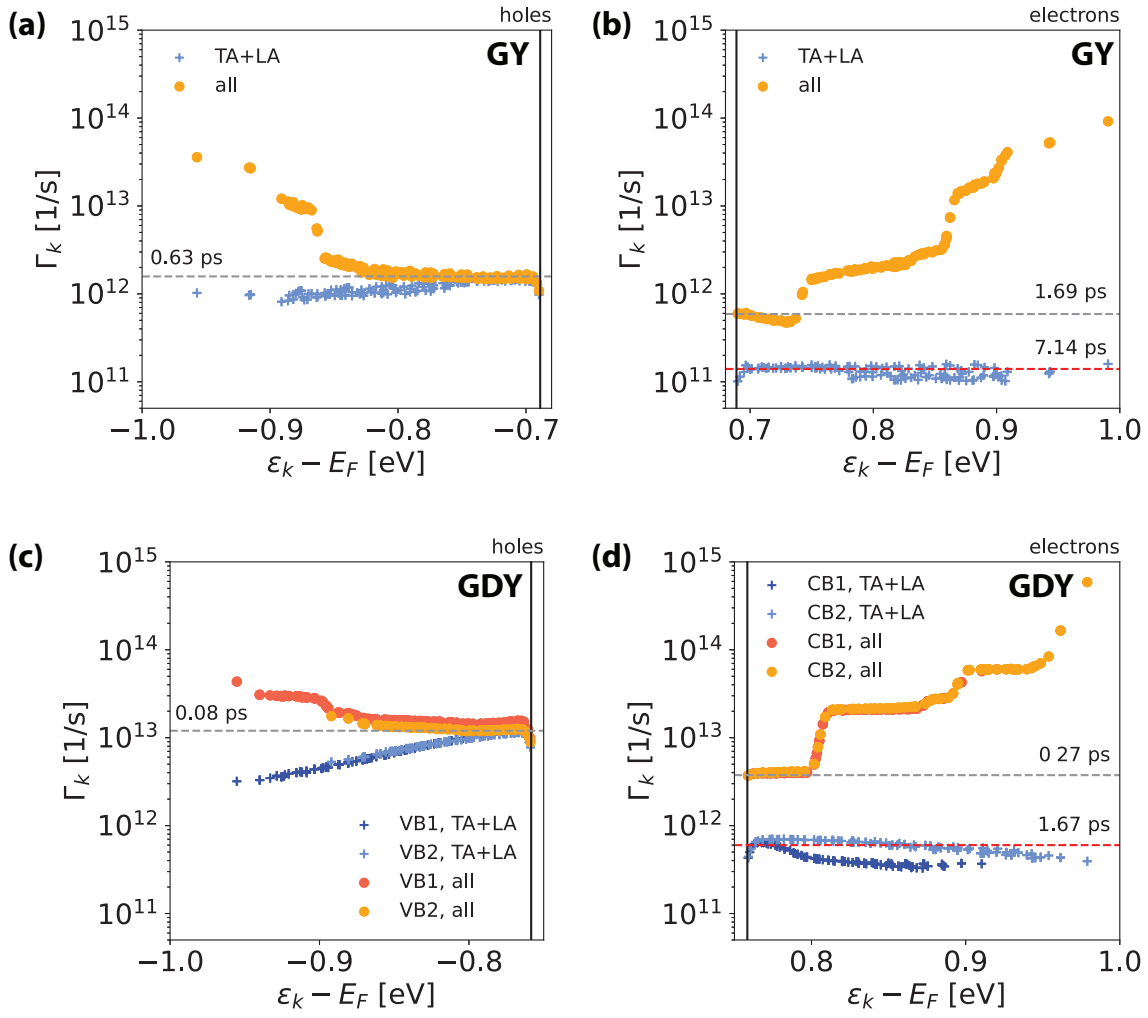

FIG. 7. The scattering rates (inverse life-times) for (a) the holes and (b) the electrons in monolayer graphyne (GY), as well as for the (c) holes and (d) electrons in monolayer graphdiyne (GDY). In this plot, scatterings were calculated at fixed temperature $T = 300$ K and fixed chemical potential within SERTA. The chemical potentials were set to the band edge values.

[1] A. R. Puigdollers, G. Alonso, and P. Gamallo, First-principles study of structural, elastic and electronic properties of α-, β- and γ-graphyne, Carbon **96**, 879 (2016).

[2] M. Long, L. Tang, D. Wang, Y. Li, and Z. Shuai, Electronic structure and carrier mobility in graphdiyne sheet and nanoribbons: Theoretical predictions, ACS Nano **5**, 2593 (2011), pMID: 21443198.

[3] B. Hourahine, B. Aradi, V. Blum, F. Bonafé, A. Buccheri, C. Camacho, C. Cevallos, M. Y. Deshaye, T. Dumitrică, A. Dominguez, S. Ehlert, M. Elstner, T. van der Heide, J. Hermann, S. Irle, J. J. Kranz, C. Köhler, T. Kowalczyk, T. Kubař, I. S. Lee, V. Lutsker, R. J. Maurer, S. K. Min, I. Mitchell, C. Negre, T. A. Niehaus, A. M. N. Niklasson, A. J. Page, A. Pecchia, G. Penazzi, M. P. Persson, J. Řezáč, C. G. Sánchez, M. Sternberg, M. Stöhr, F. Stuckenberg, A. Tkatchenko, V. W.-z. Yu, and T. Frauenheim, Dftb+, a software package for efficient approximate density functional theory based atomistic simulations, The Journal of Chemical Physics **152**, 124101 (2020).

[4] M. Gaus, A. Goez, and M. Elstner, Parametrization and benchmark of dftb3 for organic molecules, Journal of Chemical Theory and Computation **9**, 338 (2013), pMID: 26589037.

[5] M. Gaus, X. Lu, M. Elstner, and Q. Cui, Parameterization of dftb3/3ob for sulfur and phosphorus for chemical and biological applications, Journal of Chemical Theory and Computation **10**, 1518 (2014), pMID: 24803865.

[6] M. Elstner, D. Porezag, G. Jungnickel, J. Elsner, M. Haugk, T. Frauenheim, S. Suhai, and G. Seifert, Self-consistent-charge density-functional tight-binding method for simulations of complex materials properties, Phys. Rev. B **58**, 7260 (1998).

[7] V. Q. Vuong, J. Akkarapattiakal Kuriappan, M. Kubillus, J. J. Kranz, T. Mast, T. A. Niehaus, S. Irle, and M. Elstner, Parametrization and benchmark of long-range corrected dftb2 for organic molecules, Journal of Chemical Theory and Computation **14**, 115 (2018), pMID: 29232515.

[8] B. Lukose, A. Kuc, J. Frenzel, and T. Heine, On the reticular construction concept of covalent organic frameworks, Beilstein J. Nanotechnol. **1**, 60 (2010).

[9] S. Poncé, W. Li, S. Reichardt, and F. Giustino, First-principles calculations of charge carrier mobility and conductivity in bulk semiconductors and two-dimensional materials, Reports on

Progress in Physics **83**, 036501 (2020).

[10] L. D. Whalley, J. M. Frost, B. J. Morgan, and A. Walsh, Impact of nonparabolic electronic band structure on the optical and transport properties of photovoltaic materials, Phys. Rev. B **99**, 085207 (2019).

[11] C. Rudderham and J. Maassen, Analysis of simple scattering models on the thermoelectric performance of analytical electron dispersions, Journal of Applied Physics **127**, 065105 (2020).

[12] M. Lundstrom, *Fundamentals of Carrier Transport*, 2nd ed. (Cambridge University Press, 2000) pp. 14–15.